

# Study on the Pyrolysis Kinetic Behaviors of Different Vegetable-Tanned Sheepskin Leathers

by

Chaoya Ren,<sup>1</sup> Yadi Hu,<sup>1</sup> Jie Liu,<sup>1</sup> Fang Wang,<sup>1,\*</sup> Yong Lei,<sup>2</sup> Mădălina Georgiana Albu Kaya<sup>3</sup> and Keyong Tang<sup>1,\*</sup>

<sup>1</sup>School of Materials Science and Engineering, Zhengzhou University, Zhengzhou 450001, P R China

<sup>2</sup>Department of Conservation Science, Palace Museum, Beijing 100009, P R China

<sup>3</sup>Leather and Footwear Research Institute, Collagen Department, 93 Ion Minulescu, Bucharest 031215, Romania

## Abstract

The pyrolysis behaviors of leathers tanned with hydrolyzable tannins (Tara and Chestnut extracts), and condensed tannins (Quebracho and Mimosa extract) were studied by Thermogravimetric (TG) analysis in the present work. The TG/derivative thermogravimetry (DTG) results showed that the thermal stability of Tara- and Chestnut-tanned samples is poorer than that of Quebracho- and Mimosa-tanned ones. In order to study pyrolysis kinetics, TG experiments at different heating rates were carried out. Two methods of Flynn-Wall-Ozawa (FWO) and Friedman (FR) were employed to calculate the pyrolysis activation energy ( $E_a$ ) of the samples. It was found that the average  $E_a$  of the vegetable-tanned samples is located at the range of 191.7-206.1 kJ/mol. The thermodynamic parameters (pre-exponential factor, Gibbs free energy, enthalpy, and entropy) of the samples were subsequently calculated based on the average  $E_a$  by the FR method. The Gibbs free energies of the Chestnut-, Tara-, Quebracho-, and Mimosa-tanned leathers were 176.9 kJ/mol, 179.8 kJ/mol, 179.3 kJ/mol, and 178.2 kJ/mol, respectively. The difference between the average enthalpies and the  $E_a$  is less than 5 kJ/mol, which indicated that the pyrolysis process is conducive to the product formation. The mean entropy ( $\Delta S$ ) of the four vegetable-tanned samples is all positive, which suggested that the pyrolysis of the samples could easily take place. This work might provide theoretical guidance for the optimization of vegetable-tanned leather waste pyrolysis.

## Introduction

As a collagen-based composite, leather has been widely used in our daily life. Generally, leather is made from raw skins/hides by a series of processes, such as beamhouse, tanning, dressing, and finishing. Plenty of solid tannery waste is generated during these processes, i.e., trimmings, shavings, or buffing dust.<sup>1</sup> It has been reported that by processing 1 ton rawhide, 200 kg of tanned leather is obtained, while 200-250 kg of tanned waste, and 190-350 kg of non-tanned waste are generated.<sup>2</sup> Nowadays, chrome tanning with chromium (III) salts is the most commonly used method. However, the trivalent chromium in leather might be converted into hexavalent chromium, which is

toxic and harmful to the health of humans.<sup>3-4</sup> Therefore, traditional vegetable tanning has attracted more and more attention because of its environmental friendliness and plasticity.<sup>5</sup> With the increase of vegetable-tanned leather waste output, it is of great significance to reasonably deal with the vegetable-tanned leather waste for the sustainable development of the leather industry.<sup>6</sup>

So far, landfill and partial treatment are the main waste management practices of tanneries. The innovative development of treatment methods based on biology, chemistry, heat, and immobilization provided a new technical solution for the treatment of leather waste.<sup>7-10</sup> Among them, by the pyrolysis technology, the tannery solid waste could be converted into useful gas, liquid, and solid fuel. The proportion of pyrolysis product components is affected by factors such as final temperature and heating rate.<sup>11-12</sup> Therefore, it is necessary to investigate the pyrolysis kinetics of vegetable-tanned leather, by which the pyrolysis conditions could be optimized. Some reported research on pyrolysis kinetics of leather were mainly focused on the pyrolysis of chrome-tanned leather waste. Guan *et al.* investigated the pyrolysis of chromium-tanned leather shavings, and they found that the chromium-tanned leather shavings may be potential candidates for bioenergy production and carbon preparation.<sup>13</sup> The chrome-tanned leather wastes are toxic and hard-to-degrade due to the presence of hazardous chromium salts. So Zhang *et al.* studied a new way, by which the chrome-tanned leather scrap was treated to extract chromium salts, and then the pyrolysis of the acid-treated chrome-tanned leather scrap took place more easily in an inert atmosphere.<sup>14</sup> Beltrán-Prieto *et al.* found that with sodium hydroxide as the hydrolysis agent, the chromium might be easily recycled from solid leather waste in order to a produce tanning liquor.<sup>15</sup>

Liu *et al.* investigated the pyrolysis kinetics of vegetable-tanned calf leather and found that the average pyrolysis activation energy ( $E_a$ ) of vegetable-tanned leather was 241.9 kJ/mol.<sup>16</sup> Gil *et al.* studied the pyrolysis process of a mixture of the three most abundant solid wastes from vegetable tanning, including shavings, trimmings, and buffing dust, by which they found that the heating rate did not significantly affect the kinetic parameters and the weight loss.<sup>1</sup> Sebestyén *et al.* found that the thermal stability of leather tanned with hydrolyzable

\*Corresponding author email: kytangzzu@hotmail.com ; cattwm@zzu.edu.cn  
Manuscript received February 15, 2023, accepted for publication March 10, 2023.

vegetable tannins was lower than that tanned with condensed vegetable tannins.<sup>17</sup> Onem *et al.* reported that the thermal stability of leather was dependent on the types of tanning agents.<sup>18</sup> Hu *et al.* pointed out that the pyrolysis process of vegetable-tanned leather was complex and different for different types of vegetable tanning agents.<sup>19</sup> Carçote *et al.* found that the animal species used for leather making affected the thermal behaviors of the resulted leather.<sup>20</sup> However, the study of pyrolysis kinetics of vegetable-tanned leathers is still limited and mostly focused on the pyrolytic stability of calf leather. So, further studies are still needed on the pyrolysis kinetics of vegetable-tanned sheepskin leather.

In the present paper, the pyrolysis kinetics of sheepskin leather samples tanned with Chestnut, Tara, Quebracho, and Mimosa extracts were investigated by Thermogravimetry analysis (TGA), which has been proved an effective method to study the pyrolysis kinetics of materials. The purpose of this work is to comprehensively evaluate the pyrolysis kinetics and determine the difference between the sheepskin leathers tanned with different vegetable tannins. The results obtained in this paper might provide valuable guidance for the favorable treatment and reuse of solid vegetable-tanned leather waste.

## Experimental

### Sample preparation and characterization

Pickled sheepskins were provided by Henan Prosper Skin & Leather Enterprise Co. Ltd. (Jiaozuo, China). After the pH of pickled sheepskins was adjusted to 5-8 with sodium thiosulfate, tanning was done with 50 wt.% Tara, Quebracho, Chestnut, and Mimosa extracts. Sodium thiosulfate (Na<sub>2</sub>S<sub>2</sub>O<sub>3</sub>) was purchased from Tianjin Kemiou Chemical Reagent Co., Ltd. (Tianjin, China). Tara and Quebracho were purchased from Hengrongze Trading Co., Ltd. (Zhengzhou, China). Chestnut and Mimosa extracts were purchased from Bosi Chemical Co., Ltd. (Xinji, China). The percentage of the tanning agents were based on the weights of the pickled sheepskins. After being tanned for 7 days, leather samples were washed with distilled water to remove the non-reacted tanning agents and were dried at room temperature. Then, the obtained leather samples were kept in a desiccator for subsequent use.

Nicolet iS5 (Thermo Scientific, USA) Fourier transform infrared (FTIR) spectrometer was used to record the FTIR spectra at room temperature. Infrared spectrometry was performed on samples using the potassium bromide (KBr) tablet method. The spectra were collected from 4000 to 400 cm<sup>-1</sup> at a resolution of 4 cm<sup>-1</sup>.

Shrinkage temperature ( $T_s$ ) of the samples was measured by the MSW-YD4 shrinkage instrument (Sunshine Electronic Research Institute of Shanxi University of Technology, China).<sup>12,21</sup> After being immersed in water for 24 h, the samples were heated in water with a heating rate of  $2.0 \pm 0.2^\circ\text{C}/\text{min}$ . In this work, the  $T_s$  of each sample was the average of at least three measurements.

The data were repeated at least three times and expressed as mean value  $\pm$  standard deviation. Statistical differences were analyzed by one-way ANOVA and Student's t-test.  $P < 0.05$  was considered as statistical significance.

### Thermogravimetric analysis (TGA)

Pyrolysis measurements were carried out using a TGA/DSC1 (METTLER TOLEDO, Switzerland). Samples of 5-10 mg were placed into an open aluminum crucible. The temperature was increased from 30°C to 600°C in a nitrogen atmosphere with a gas flow rate of 40 mL/min. The pyrolysis tests of vegetable-tanned samples were performed at heating rates of 10, 30, and 50°C/min, respectively.

### Pyrolysis kinetic analysis

In the iso-conversional methods, the pyrolysis process of solid materials can be expressed by Equation 1.<sup>22</sup>

$$\frac{d\alpha}{dt} = K(T)f(\alpha) \quad (1)$$

The  $K(T)$  in Equation 1 represents the reaction rate constant, which can be defined as Equation 2.

$$K(T) = A \exp\left(-\frac{E}{RT}\right) \quad (2)$$

From Equation 1 and 2, the Equation 3 is obtained.

$$\frac{d\alpha}{dt} = A \exp\left(-\frac{E}{RT}\right) f(\alpha) \quad (3)$$

Where  $A$  is the pre-exponential factor,<sup>23</sup>  $E_a$  is the activation energy,  $R$  is the gas constant (8.314 J/Kmol),  $T$  is the absolute temperature,  $f(\alpha)$  is the mechanism function, and  $\alpha$  is the conversion, as defined in Equation 4.

$$\alpha = \frac{m_0 - m_t}{m_0 - m_f} \quad (4)$$

Where  $m_0$  is the initial sample weight, and  $m_t$  is the sample weight at the end of the pyrolysis;  $m_t$  is the sample weight at the time  $t$  (given in min).

The thermal degradation process is temperature dependent, which increases with time at a fixed heating rate. Thus, the heating rate  $\beta = dT/dt$  was introduced to Equation 3 to yield Equation 5 for the non-isothermal thermal degradation process of solid materials.

$$\beta \frac{d\alpha}{dt} = A \exp\left(-\frac{E}{RT}\right) f(\alpha) \quad (5)$$

Integrating Equation 5 gives Equation 6:

$$g(\alpha) = \int_0^\alpha \frac{d\alpha}{f(\alpha)} = \frac{A}{\beta} \int_0^T \exp\left(-\frac{E}{RT}\right) dT = \frac{AE_a}{\beta R} P(x) \quad (6)$$

Since the  $P(x)$  in Equation 6 has no explicit solution, the Doyle approximation was used by Flynn-Wall-Ozawa (FWO) method to

determine the  $E_a$ .<sup>24</sup> The FWO equation is shown in Equation 7.<sup>23,25</sup> The  $E_a$  was calculated from the slope of the  $\ln \beta$  vs.  $1000/T$ .

$$\ln(\beta) = \ln \frac{AE_a}{g(\alpha)R} - 5.331 - 1.052 \frac{E_a}{RT} \quad (7)$$

Friedman (FR) method was also applied in this work to determine the  $E_a$  with no information of pyrolysis mechanism needed in advance, which is defined by Equation 8.<sup>26</sup> Then,  $E_a$  can be obtained by the slope of  $\ln(\beta \cdot d\alpha/dt)$  vs.  $1000/T$ .

$$\ln(\beta \frac{d\alpha}{dt}) = \ln[Af(\alpha)] - \frac{E_a}{RT} \quad (8)$$

## 2.4 Thermodynamic parameters

The activation energies obtained from the above mentioned iso-conversional models were used to calculate the pre-exponential factor ( $A$ ) in the Arrhenius equation (Equation 1 based on Equation 9).  $T_m$  is the peak temperature of the DTG curve.

$$A = \beta E_a \exp\left(\frac{E_a}{RT_m}\right) / (RT_m^2) \quad (9)$$

The thermodynamic parameters including the enthalpy change ( $\Delta H$ ), Gibbs free energy change ( $\Delta G$ ), and entropy change ( $\Delta S$ ) can be calculated by the following equations:<sup>27-28</sup>

$$\Delta H = E_a - RT \quad (10)$$

$$\Delta G = E_a + RT_m \ln\left(\frac{K_b T_m}{hA}\right) \quad (11)$$

$$\Delta S = \frac{\Delta H - \Delta G}{T_m} \quad (12)$$

Where  $K_b$  is the Boltzmann constant ( $1.381 \times 10^{-23}$  J/k), and  $h$  is the Planck constant ( $6.626 \times 10^{-34}$  J.S).

## Results and Discussion

### Characterization of different tanned leather samples

As a very useful and popular instrument, FTIR is sensitive to protein structure information. The ATR-FTIR spectra of the untanned and the Chestnut-, Tara-, Quebracho-, and Mimosa-tanned leather samples are shown in Figure 1. For all the samples, the characteristic absorption bands of collagen could be obviously observed, such as amide A ( $\nu_{(N-H)} \approx 3310 \text{ cm}^{-1}$ ), amide B ( $\nu_{(N-H)} \approx 3077 \text{ cm}^{-1}$ ),  $-\text{CH}_3$  ( $\nu_{\text{as}(C-H)} \approx 2917 \text{ cm}^{-1}$ ),  $-\text{CH}_2$  ( $\nu_{\text{as}(C-H)} \approx 2848 \text{ cm}^{-1}$ ), amide I ( $\nu_{(C=O)} \approx 1637 \text{ cm}^{-1}$ ), amide II ( $\delta_{(N-H)}$  and  $\nu_{(C-N)} \approx 1544 \text{ cm}^{-1}$ ), and amide III ( $\delta_{(N-H)}$  and  $\nu_{(C-N)} \approx 1234 \text{ cm}^{-1}$ ).<sup>12,29-31</sup> In addition to the characteristic peaks of collagen, the bands of Chestnut and Tara were also observed, the  $\nu_{(C=O)} \approx 1720 \text{ cm}^{-1}$  and  $\nu_{(C=C)} \approx 1450 \text{ cm}^{-1}$ .<sup>32</sup>

The shrinkage temperature ( $T_s$ ) of the samples is shown in Figure 2. The  $T_s$  of untanned sample is  $58.8 \pm 0.9^\circ\text{C}$ . After tanning, the crosslinking degree of skin collagen fiber increases, which is manifested by the increase of  $T_s$ . The high  $T_s$  indicates good hydrothermal stability and tanning effect.<sup>12,33</sup> In Figure 2, the  $T_s$  of the Chestnut-, Tara-, Quebracho-, and Mimosa-tanned leather samples are  $78.7 \pm 0.4^\circ\text{C}$ ,  $72.7 \pm 1.7^\circ\text{C}$ ,  $81.3 \pm 0.8^\circ\text{C}$ , and  $79.7 \pm 0.9^\circ\text{C}$ , respectively. The hydrothermal stability of the samples tanned with condensed tannins (Quebracho, Mimosa) are higher than those tanned with hydrolyzable tannins (Chestnut, Tara). For Quebracho and Mimosa extracts, all aromatic rings are linked by carbon-carbon bonds, by which a stable link-lock structure with collagen is formed. For Chestnut and Tara, however, the polyols and phenolic acids in them are linked by ester bonds. Ester bonds are easier to break than carbon-carbon bonds. The  $T_s$  of Quebracho- and Mimosa-tanned leather sample are higher than those of leathers tanned with Chestnut and Tara. The molecules of Tara have linear structure with

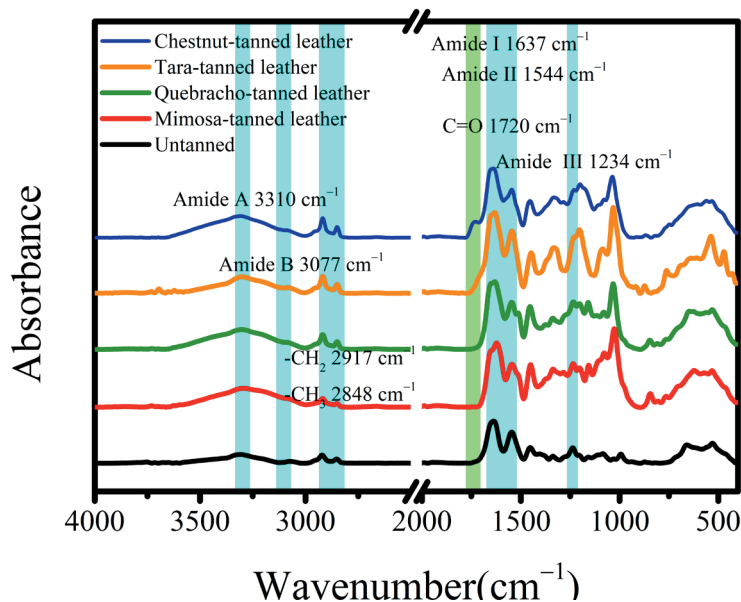
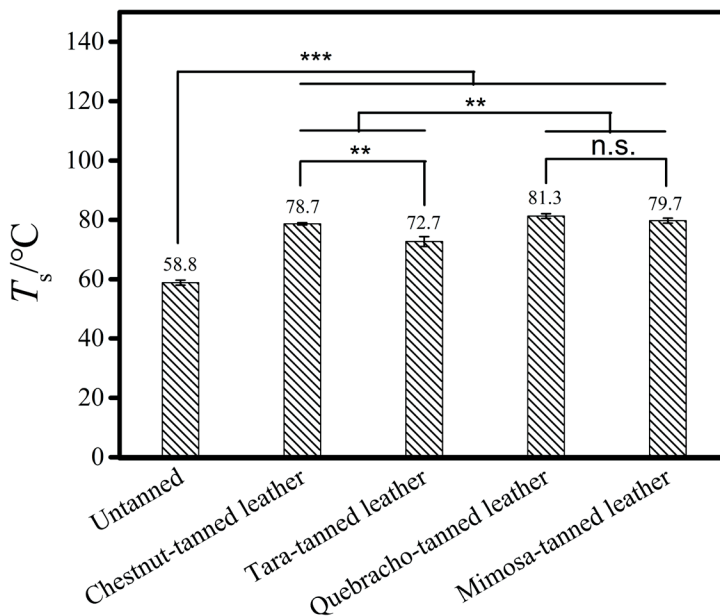


Figure 1. ATR-FTIR spectra of the untanned and the Chestnut-, Tara-, Quebracho-, and Mimosa-tanned sheepskin leather samples



**Figure 2.** Shrinkage temperatures of the untanned sample and the Chestnut-, Tara-, Quebracho-, and Mimosa-tanned samples. The “n.s.” indicates no significant difference, \*\* $P < 0.01$ , \*\*\* $P < 0.001$ .

poor stiffness, while those of Chestnut have body structure with good stiffness. The tanning agent with good stiffness might make it difficult for the tanned collagen fibers to move relatively, resulting in higher  $T_s$  of the tanned leather. Therefore, the  $T_s$  of Chestnut-tanned leather is higher than that of Tara-tanned leather.

#### TG/DTG analysis

Figure 3 shows the TG/DTG curves of the samples at a heating rate of 10°C/min. The TG curves showed two successive weight loss trends in the temperature ranges of 30–150°C and 150–450°C. Similar weight loss temperature range appeared in the TG curves of samples before and after vegetable tanning. The final residual

mass percentage of the untanned sample is 25.98 wt.%, which was increased to 36.97 wt.%, 31.46 wt.%, 36.55 wt.%, and 37.59 wt.% for Chestnut-, Tara-, Quebracho-, and Mimosa-tanned leather samples, respectively. Compared with chrome-tanned leather (28.4 wt.%), the final residual ratio of vegetable-tanned leather is high.<sup>14</sup> Thus, the vegetable-tanned leather wastes have potential as a raw material for bio-char production.

According to the DTG curves of the samples, the pyrolysis process of all the samples could be divided into three distinct stages, namely, the dehydration stage (stage 1, 30–150°C), the fast devolatilization component stage (stage 2, 150–450°C), and the carbonization stage

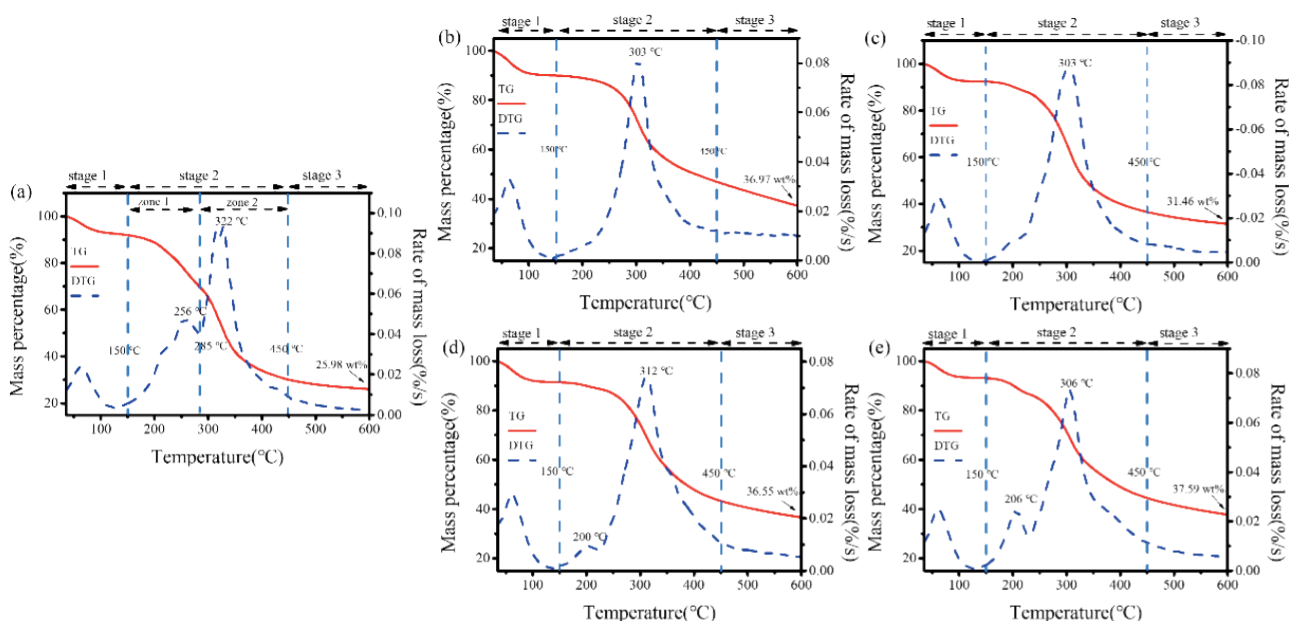


**Figure 3.** TG/DTG curves of (a) untanned, (b) Chestnut-tanned, (c) Tara-tanned, (d) Mimosa-tanned, and (e) Quebracho-tanned samples.

(stage 3, 450-600°C). Stage 1 is mainly related to release of moisture and absorbed water in the samples, and the weight loss of the untanned sample at this stage is 7.47 wt.%, based on the original weight of the sample. Approximately 8.00 wt.% weight loss was found below 150°C for the samples tanned with Chestnut, Tara, Quebracho, and Mimosa. Stage 2 is a fast devolatilization (150-450°C), which is the main pyrolysis stage of the samples. From Figure 3 (a), the stage 2 of the untanned sample was composed of two weight loss zones (Zone 1 and Zone 2), and the weight loss in Zone 1 and Zone 2 were 22.94 wt.% and 39.50 wt.%, respectively. At stage 2, the total weight loss of the untanned sample was 62.44 wt.%. Vegetable tanning decreases the weight loss of the samples at this stage. The weight loss of the Mimosa- and Quebracho-tanned leather sample is around 49.00 wt.%. The weight loss of Tara-tanned leather is about 57.00 wt.%, greater than that of Chestnut-tanned leather (about 44.00 wt.%). The gases released by the pyrolysis of vegetable-tanned samples in nitrogen atmosphere are CO<sub>2</sub>, H<sub>2</sub>O, NH<sub>3</sub>, phenol derivatives, and nitriles.<sup>19, 34</sup> Stage 3 is the carbonization stage (450-600°C), and the weight loss of all samples slowly increases with increasing the temperature. According to the DTG curves of the untanned sample and the vegetable-tanned leather samples, the difference between the dehydration stage and the carbonization stage is nearly negligible, while some differences do exist in the fast devolatilization stage. In Figure 3 (a), two peaks appeared at 256°C and 322°C in the fast devolatilization stage of the untanned sample. The pyrolysis peak at 256°C may be due to the partial hydrolysis of the pickled sheepskin, and the one around 322°C can be classified as the peak of collagen.<sup>16, 35-36</sup> For the vegetable-tanned leather, the main pyrolysis takes place at stage 2. However, there appeared a small peak or shoulder at 200°C as shown in Figure 3 (b-e), which might be because of the partial pyrolysis of tannins.<sup>17</sup>

For the maximum pyrolysis rate (DTG<sub>max</sub>), the DTG<sub>max</sub> of the Chestnut-, Tara-, Quebracho-, and Mimosa-tanned leather samples were all lower than that of the untanned sample. So, vegetable tanning might be able to decrease the DTG<sub>max</sub>. The DTG<sub>max</sub> of sample tanned with hydrolyzable tanning agents of Chestnut and Tara is higher than those tanned with condensed tanning agents of Quebracho and Mimosa. The temperature of DTG<sub>max</sub> ( $T_{peak}$ ) of the samples tanned with Chestnut, Tara, Quebracho, and Mimosa are 303°C, 303°C, 312°C, and 306°C, respectively. All the vegetable-tanned leather samples had lower  $T_{peak}$  than the untanned sample (322°C). The  $T_{peak}$  of the leathers tanned with hydrolysis tanning agents of Chestnut and Tara is significantly lower than those tanned with condensed tannings of Quebracho and Mimosa. The condensed tanning agent might provide leathers with higher thermal stability than hydrolysis tanning agent.

### Pyrolysis kinetic analysis

Thermodynamic parameters are critically important in order to know the pyrolysis mechanism of materials. By the model-free iso-conversional methods, the thermodynamic parameters can be calculated with no need to build an accurate reaction model.<sup>16</sup> TG/DTG curves for the pyrolysis of untanned and four vegetable-tanned leather samples at three different heating rates (10, 30, 50°C/min) are shown in Figure 4. With the increase of temperature, the curves of the samples slightly move towards high temperature. The shape of the curves does not change significantly, indicating that the heating rate does not affect the pyrolysis mechanism of the samples. The iso-conversional methods were applied to calculate the thermodynamic parameters. Since stage 2 (150-450°C) corresponds to the main pyrolysis process, the TG curve was transformed into the form of conversion and temperature ( $\alpha$  vs.  $T$ ) to study the kinetics of this stage, as shown in Figure 5 (a, d, g, j, m).

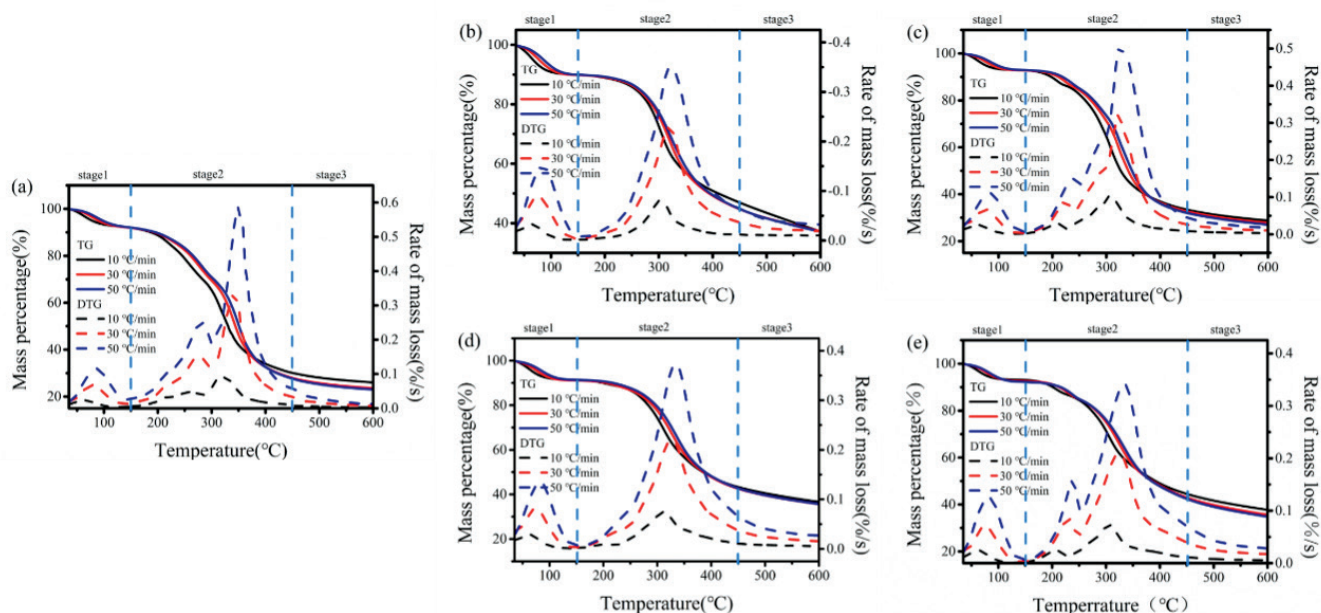


**Figure 4.** TG/DTG curves of the samples at different heating rates: (a) untanned, (b) Chestnut-tanned, (c) Tara-tanned, (d) Mimosa-tanned, and (e) Quebracho-tanned samples.

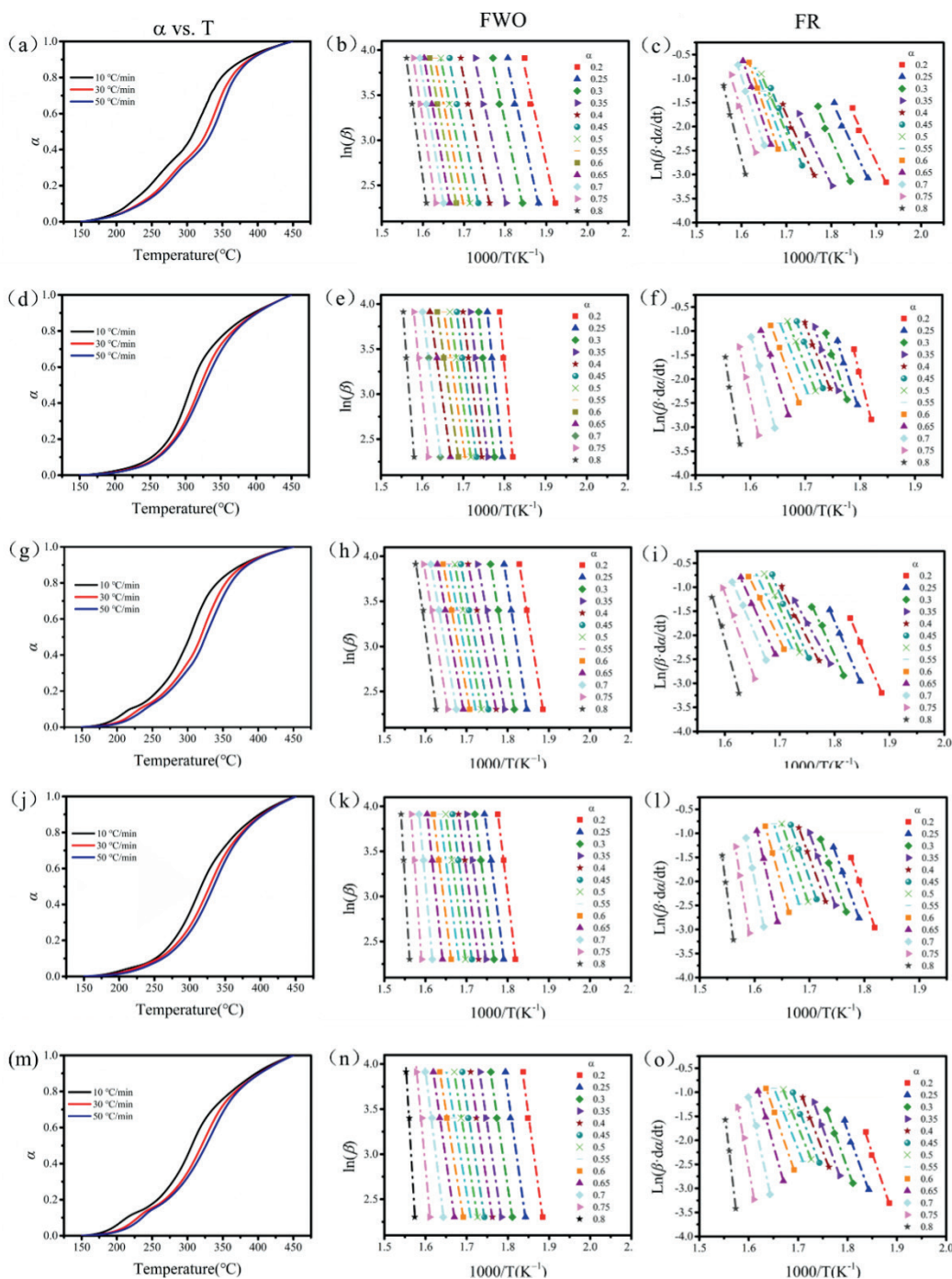


**Figure 5.** Conversion ( $\alpha$ ) curves with temperature; plots of  $\ln \beta$  vs.  $1000/T$  and  $\ln(\beta-d\alpha/dT)$  vs.  $1000/T$  by methods of FWO and FR: (a, b, c) untanned, (d, e, f) Chestnut-tanned, (g, h, i) Tara-tanned, (j, k, l) Quebracho-tanned, and (m, n, o) Mimosa-tanned samples.

In this work, both methods of FWO and FR were used to calculate the main thermodynamic parameters including  $E_a$ . The relations of  $\ln(\beta)$  vs.  $1000/T$  (FWO) (Figure 5 (b, e, h, k, n)) and  $\ln(\beta-d\alpha/dT)$  vs.  $1000/T$  (Figure 5 (c, f, i, l, o)) (FR) were obtained according to Equation 7 and Equation 8. The slopes of the lines were obtained by the method of ordinary least squares, which were used to calculate the  $E_a$ . In order to know the dependency of  $E_a$  on  $\alpha$ , the range of conversion rate was chosen from 0.2 to 0.8 with a step length of 0.05.

The  $R^2$  of four vegetable-tanned leather samples was above 0.99, and the  $R^2$  of the untanned sample was above 0.98, indicating the good accuracy and reliability of  $E_a$ , as well as the reasonableness of the model studied here.<sup>36</sup>

$E_a$  is defined as the minimum energy needed for the reaction.<sup>37</sup> In Figure 6 (a, c, e, g, i) and Table I, the  $E_a$  of untanned sample and different vegetable-tanned leather sample showed obvious

fluctuation of conversion, indicating that their pyrolysis is unlikely to be dominated by a single-step mechanism.<sup>23</sup> In Figure 6 (a), the  $E_\alpha$  of the untanned samples increases gradually with the increase of conversion. Figure 6 (c) showed that the  $E_\alpha$  of Chestnut-tanned leather sample decreases first in the conversion range of 0.2-0.5 and then, gradually increases with further increasing the conversion. Compared to the Chestnut-tanned leather sample, the  $E_\alpha$  of Tara-tanned leather sample (Figure 6 (e)) showed complex fluctuation with the increase of conversion. In Figure 6 (g, i), the  $E_\alpha$  of Quebracho- and Mimosa-tanned leather samples showed the same trend with the increase of conversion, although the specific value of  $E_\alpha$  at different conversions is dissimilar. Vyazovkin *et al.* proposed that the pyrolysis of materials was a complex reaction process. At the absolute deviation  $\varepsilon_E$  ( $\varepsilon_E = |E_\alpha - E_0| \times 100 / E_0$ , %) of less than 30%, the pyrolysis reaction was considered a single reaction.<sup>23</sup> In Figure 6 (b, d, f), the average  $\varepsilon_E$  of the untanned sample, Chestnut- and Tara-tanned leather samples were all less than 30%, suggesting a one-step reaction. For the Quebracho- and Mimosa-tanned leather samples, the average  $\varepsilon_E$  was close to 30%, as shown in Figure 6 (h, j). The  $\varepsilon_E$  values of untanned sample and the Chestnut- and Tara-tanned leather samples are higher than 30% at the  $\alpha$  of more than 0.8, whereas the  $\varepsilon_E$  values of Quebracho- and Mimosa-tanned leather samples are higher than 30% at the  $\alpha$  of more than 0.75. The possible reason is that more unstable free radicals might be generated in the pyrolysis reactions at high conversions, which might cause more side reactions to take place.<sup>38</sup> So there should be secondary reactions between the gaseous products and pyrolyzed char, and the complexity of the pyrolysis was indicated.<sup>16, 35</sup>

The mean  $E_\alpha$  is in the range of 191.7-206.1 kJ/mol for untanned sample. After being vegetable-tanned, the mean  $E_\alpha$  of samples is increased. Among them, the  $E_\alpha$  of the Quebracho-tanned leather is the highest (333.2-363.8 kJ/mol), followed by those of the Chestnut-(310.0-315.3 kJ/mol) and Mimosa-tanned (282.7-309.0 kJ/mol) leather samples. The  $E_\alpha$  of Tara-tanned leather sample (209.2-220.6 kJ/mol) is the lowest among the four vegetable-tanned leathers samples.

The introduction of different tanning agents in the leather causes the differences in the  $E_\alpha$  of vegetable-tanned leathers due to their cross-linking (stabilization) effect. Thus, it is necessary to discuss the influence of tanning agents on leather. Compared with Tara-tanned leather samples, the  $E_\alpha$  of Chestnut-tanned samples is higher, which may be because of the different molecular structure. The Chestnut tannins are ellagitannins, and Tara tannins are gallotannins.<sup>39</sup> The  $E_\alpha$  of Quebracho- (333.2-363.8 kJ/mol) and Mimosa-tanned (282.7-309.0 kJ/mol) sheepskin leather is higher than that of Mimosa-tanned calf leather (250.0-272.7 kJ/mol),<sup>19</sup> but lower than those of chrome-tanned calf leather (348.8-391.8 kJ/mol).<sup>13</sup> The  $E_\alpha$  of vegetable-tanned leather in this paper was higher than that of *Chlorella vulgaris* (156.2-158.1 kJ/mol),<sup>27</sup> as well as those agricultural waste, such as rice husk (48.6-54.2 kJ/mol),<sup>40</sup> peanut husk (96.9-109.9 kJ/mol),<sup>41</sup> and wheat straw (130.0-175.0 kJ/mol).<sup>42</sup>

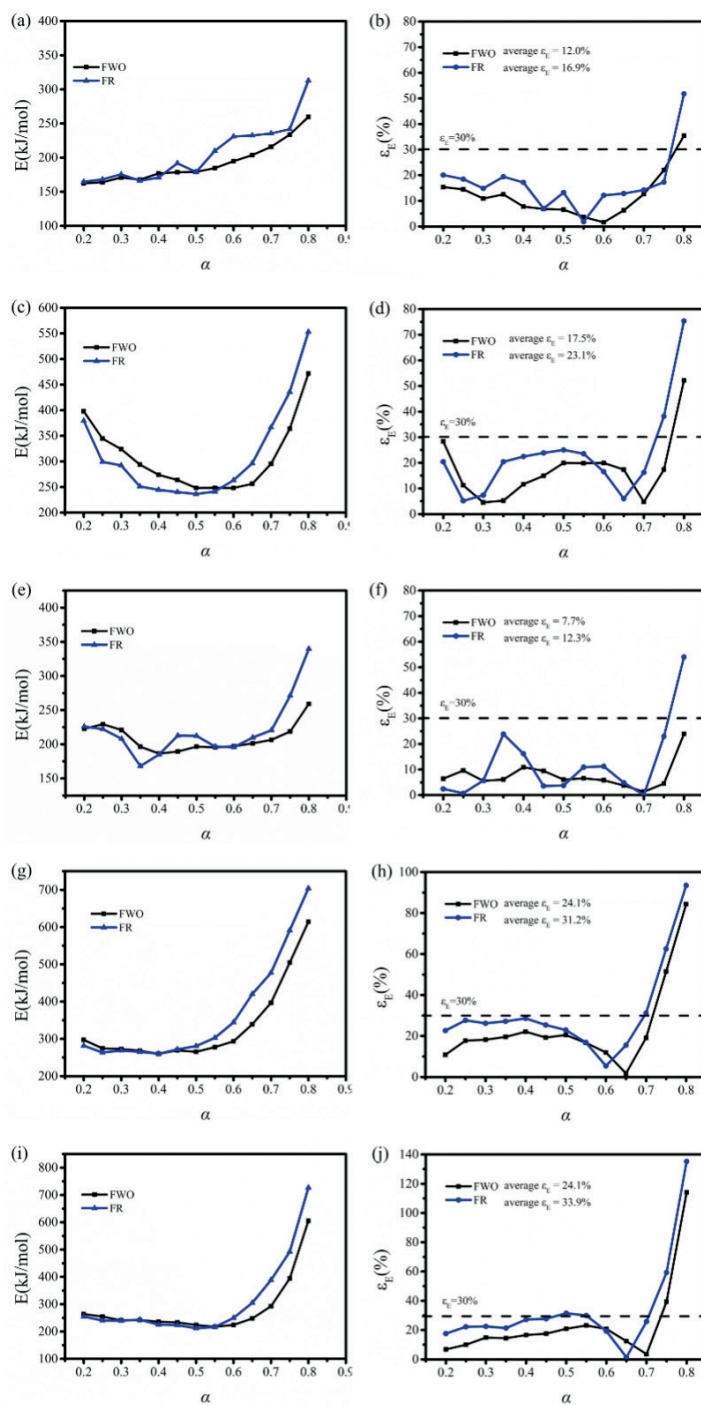


**Figure 6.** The relationship between  $E_\alpha$  and absolute deviation ( $\varepsilon_E$ ) of (a, b) untanned, (c, d) Chestnut-tanned, (e, f) Tara-tanned, (g, h) Quebracho-tanned, and (i, j) Mimosa-tanned samples with conversion ( $\alpha$ ) by FWO and FR methods.

**Table I**  
**Pyrolysis activation energy ( $E_a$ , kJ/mol) by methods of FWO and FR for the samples**

| $\alpha$ | Untanned sample |                |       |                | Chestnut-tanned sample |                |       |                | Tara-tanned sample |                |       |                | Quebracho-tanned sample |                |       |                | Mimosa-tanned sample |                |       |                |
|----------|-----------------|----------------|-------|----------------|------------------------|----------------|-------|----------------|--------------------|----------------|-------|----------------|-------------------------|----------------|-------|----------------|----------------------|----------------|-------|----------------|
|          | FWO             | R <sup>2</sup> | FR    | R <sup>2</sup> | FWO                    | R <sup>2</sup> | FR    | R <sup>2</sup> | FWO                | R <sup>2</sup> | FR    | R <sup>2</sup> | FWO                     | R <sup>2</sup> | FR    | R <sup>2</sup> | FWO                  | R <sup>2</sup> | FR    | R <sup>2</sup> |
| 0.2      | 162.3           | 0.981          | 164.8 | 0.984          | 397.8                  | 0.997          | 379.7 | 0.997          | 222.6              | 0.999          | 226.0 | 0.999          | 297.2                   | 0.999          | 281.5 | 0.999          | 263.7                | 0.994          | 254.8 | 0.993          |
| 0.25     | 164.0           | 0.988          | 168.1 | 0.990          | 344.6                  | 0.999          | 299.2 | 0.996          | 229.3              | 0.999          | 222.2 | 0.999          | 274.2                   | 0.999          | 263.2 | 0.999          | 254.7                | 0.993          | 240.4 | 0.993          |
| 0.3      | 170.9           | 0.988          | 175.6 | 0.993          | 324.0                  | 0.995          | 292.2 | 0.994          | 220.8              | 0.999          | 208.0 | 0.996          | 272.6                   | 0.999          | 268.6 | 0.999          | 240.9                | 0.998          | 239.7 | 0.998          |
| 0.35     | 167.7           | 0.994          | 166.2 | 0.997          | 293.8                  | 0.998          | 251.1 | 0.990          | 196.4              | 0.998          | 168.0 | 0.999          | 268.1                   | 0.999          | 265.1 | 0.999          | 242.0                | 0.997          | 243.1 | 0.998          |
| 0.4      | 176.9           | 0.993          | 170.7 | 0.991          | 273.9                  | 0.998          | 244.6 | 0.995          | 186.3              | 0.999          | 184.9 | 0.992          | 259.6                   | 0.999          | 259.8 | 0.999          | 236.0                | 0.996          | 225.2 | 0.999          |
| 0.45     | 178.6           | 0.995          | 191.8 | 0.999          | 263.8                  | 0.997          | 240.2 | 0.999          | 189.4              | 0.999          | 212.7 | 0.995          | 269.1                   | 0.999          | 271.6 | 0.999          | 233.3                | 0.997          | 223.4 | 0.998          |
| 0.5      | 179.2           | 0.999          | 178.9 | 0.999          | 248.2                  | 0.999          | 236.5 | 1.000          | 196.5              | 0.999          | 212.3 | 0.999          | 265.0                   | 0.999          | 280.4 | 0.999          | 223.8                | 0.999          | 211.8 | 0.999          |
| 0.55     | 184.6           | 0.998          | 209.8 | 0.999          | 248.5                  | 0.999          | 241.1 | 1.000          | 195.5              | 0.996          | 196.5 | 0.996          | 277.6                   | 0.999          | 302.6 | 0.999          | 217.4                | 1.000          | 216.6 | 0.999          |
| 0.6      | 194.7           | 0.999          | 231.1 | 0.999          | 248.2                  | 0.999          | 263.3 | 0.999          | 197.0              | 0.999          | 195.7 | 0.999          | 293.4                   | 0.999          | 344.2 | 0.999          | 224.2                | 1.000          | 249.5 | 0.999          |
| 0.65     | 203.7           | 0.999          | 232.5 | 0.999          | 256.3                  | 0.999          | 296.5 | 0.994          | 201.3              | 0.999          | 209.8 | 0.998          | 338.9                   | 0.999          | 420.1 | 0.999          | 247.8                | 1.000          | 304.8 | 0.999          |
| 0.7      | 215.9           | 0.998          | 235.4 | 0.997          | 295.3                  | 0.999          | 366.5 | 0.999          | 206.4              | 0.999          | 220.4 | 0.999          | 396.7                   | 0.999          | 477.3 | 0.999          | 292.6                | 0.996          | 388.6 | 0.992          |
| 0.75     | 233.8           | 0.999          | 241.7 | 0.983          | 363.6                  | 0.999          | 435.7 | 1.000          | 218.6              | 0.999          | 271.2 | 0.997          | 504.5                   | 0.999          | 591.1 | 0.998          | 394.0                | 0.990          | 492.3 | 0.993          |
| 0.8      | 259.7           | 0.998          | 312.8 | 0.997          | 471.6                  | 0.996          | 553.0 | 0.992          | 259.2              | 0.995          | 339.7 | 0.992          | 614.3                   | 0.999          | 703.9 | 0.999          | 605.3                | 0.994          | 726.7 | 0.998          |
| Mean     | 191.7           |                | 206.1 |                | 310.0                  |                | 315.4 |                | 209.2              |                | 220.6 |                | 333.2                   |                | 363.8 |                | 282.7                |                | 309.0 |                |

**Table II**  
**Pre-exponential factor ( $A$ , min<sup>-1</sup>) by the FR methods of Chestnut-, Tara-, Quebracho-, and Mimosa-tanned samples**

| $\alpha$ | Untanned              | Chestnut-tanned       | Tara-tanned           | Quebracho-tanned      | Mimosa-tanned         |
|----------|-----------------------|-----------------------|-----------------------|-----------------------|-----------------------|
| 0.2      | $1.63 \times 10^{11}$ | $3.66 \times 10^{31}$ | $1.79 \times 10^{17}$ | $1.33 \times 10^{22}$ | $8.68 \times 10^{19}$ |
| 0.25     | $3.25 \times 10^{11}$ | $1.45 \times 10^{24}$ | $8.02 \times 10^{16}$ | $2.89 \times 10^{20}$ | $4.15 \times 10^{18}$ |
| 0.3      | $1.53 \times 10^{12}$ | $3.29 \times 10^{23}$ | $3.96 \times 10^{15}$ | $8.92 \times 10^{20}$ | $3.59 \times 10^{18}$ |
| 0.35     | $2.17 \times 10^{11}$ | $5.28 \times 10^{19}$ | $7.97 \times 10^{11}$ | $4.30 \times 10^{20}$ | $7.43 \times 10^{18}$ |
| 0.4      | $5.62 \times 10^{11}$ | $1.33 \times 10^{19}$ | $2.93 \times 10^{13}$ | $1.43 \times 10^{20}$ | $1.65 \times 10^{17}$ |
| 0.45     | $4.42 \times 10^{13}$ | $5.23 \times 10^{18}$ | $1.09 \times 10^{16}$ | $1.68 \times 10^{21}$ | $1.14 \times 10^{17}$ |
| 0.5      | $3.07 \times 10^{12}$ | $2.36 \times 10^{18}$ | $9.82 \times 10^{15}$ | $1.06 \times 10^{22}$ | $9.68 \times 10^{15}$ |
| 0.55     | $1.86 \times 10^{15}$ | $6.36 \times 10^{18}$ | $3.46 \times 10^{14}$ | $1.09 \times 10^{24}$ | $2.65 \times 10^{16}$ |
| 0.6      | $1.50 \times 10^{17}$ | $7.06 \times 10^{20}$ | $2.95 \times 10^{14}$ | $6.40 \times 10^{27}$ | $2.88 \times 10^{19}$ |
| 0.65     | $2.03 \times 10^{17}$ | $8.12 \times 10^{23}$ | $5.82 \times 10^{15}$ | $4.72 \times 10^{34}$ | $3.41 \times 10^{24}$ |
| 0.7      | $3.68 \times 10^{17}$ | $2.26 \times 10^{30}$ | $5.55 \times 10^{16}$ | $6.76 \times 10^{39}$ | $1.57 \times 10^{32}$ |
| 0.75     | $1.34 \times 10^{18}$ | $4.99 \times 10^{36}$ | $2.53 \times 10^{21}$ | $1.22 \times 10^{50}$ | $4.48 \times 10^{41}$ |
| 0.8      | $3.02 \times 10^{24}$ | $2.74 \times 10^{47}$ | $4.64 \times 10^{27}$ | $1.70 \times 10^{60}$ | $9.09 \times 10^{62}$ |

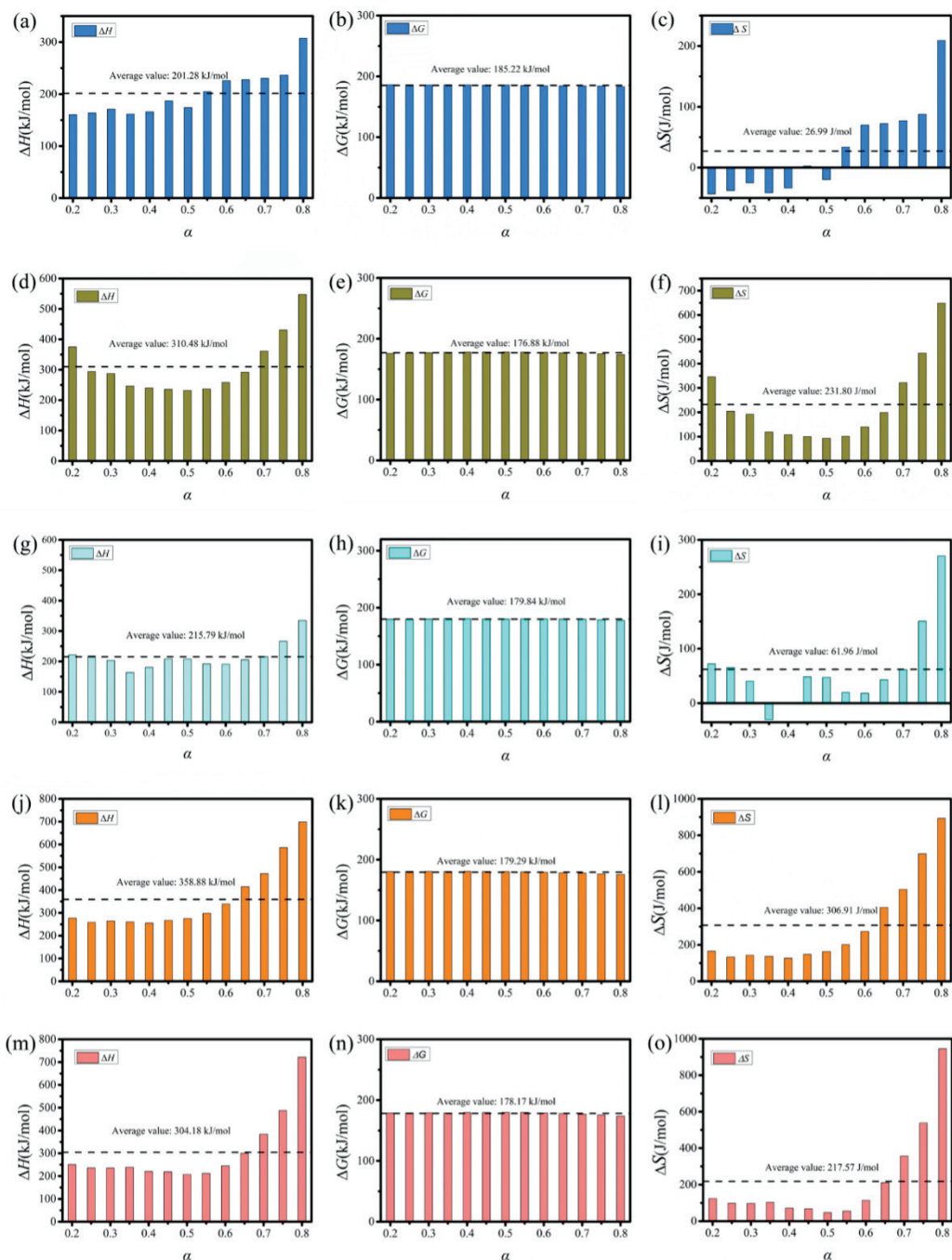


**Figure 7.** Thermodynamic parameters ( $\Delta H$ ,  $\Delta G$ , and  $\Delta S$ ) at various conversion ( $\alpha$ ) of (a, b, c) untanned, (d, e, f) Chestnut-tanned, (g, h, i) Tara-tanned, (j, k, l) Quebracho-tanned, and (m, n, o) Mimosa-tanned samples.

So vegetable-tanned leather waste might be co-pyrolyzed with several other biomass resources.

The differential FR method is more accurate than the integral FWO method when the  $E_a$  varies greatly with conversion.<sup>43</sup> So the FR method was used in this paper to calculate the thermodynamic parameters including pre-exponential factor ( $A$ ), enthalpy ( $\Delta H$ ), entropy ( $\Delta S$ ), and Gibbs free energy ( $\Delta G$ ). The thermodynamic parameters obtained are shown in Table II and Figure 7. The pre-exponential factor ( $A$ ) indicates the degree of collision per minute. The value of  $A$  represents the complexity of the chemical reaction.

The  $A$  for untanned sample is located in the range from  $10^{11}$  to  $10^{24}$ . After vegetable tanning, the range of  $A$  for the Tara-tanned leather samples is increased to  $10^{11}$ - $10^{27}$ . The values of  $A$  for Chestnut-tanned leather ( $10^{18}$ - $10^{47}$ ), Mimosa-tanned leather ( $10^{15}$ - $10^{62}$ ), and Quebracho-tanned leather ( $10^{20}$ - $10^{60}$ ) were all greater and distributed over a wider range. In addition, the trend of  $A$  is similar to that of  $E_a$ .<sup>44</sup> While the lower  $A$ -values ( $< 10^9$  s<sup>-1</sup>) show largely a surface reaction, the higher ones ( $\geq 10^9$  s<sup>-1</sup>) show a complex reaction.<sup>45</sup> In Table II, the  $A$ -values for all the samples obtained by the FR method are greater than  $10^9$  s<sup>-1</sup>. So the complexity of the reaction process was clearly indicated.<sup>46</sup>

$\Delta H$  is an important parameter of thermodynamics related to the energy consumed in the conversion of products such as gas and carbon during the pyrolysis reaction. In Figure 7, the  $\Delta H$  of Chestnut-tanned sample (d, 310.48 kJ/mol), Quebracho-tanned sample (j, 358.88 kJ/mol), and Mimosa-tanned sample (m, 304.18 kJ/mol) were higher than the Tara-tanned sample (g, 215.79 kJ/mol) and untanned sample (a, 201.28 kJ/mol). This can be explained by the fact that more energy is needed to destroy the body structure of the samples. During pyrolysis,  $\Delta H$  and  $E_a$  have the similar tendency. A slight difference ( $\sim 5$  kJ/mol) between  $\Delta H$  and  $E_a$  was found, which indicated that the pyrolysis could easily take place.<sup>41, 47</sup> The positive value of  $\Delta H$  suggested that the pyrolysis is an endothermic reaction.

The  $\Delta G$  represents the increase in total energy of the reaction during the formation of the activated complex.<sup>48-49</sup> The average  $\Delta G$  of untanned sample is 185.2 kJ/mol (Figure 7 (b)). The average  $\Delta G$  of Chestnut- and Tara-tanned leather samples are 176.9 kJ/mol and 179.8 kJ/mol, respectively (Figure 7 (e, h)), while those for Quebracho- and Mimosa-tanned leather samples are 179.3 kJ/mol, and 178.2 kJ/mol respectively (Figure 7(k, n)). Compared with the untanned sample, the  $\Delta G$  of the four vegetable-tanned leathers were all decreased, with the Chestnut-tanned sample of the lowest. All the  $\Delta G$  values are positive, indicating non-spontaneous, endothermic and energy absorbing for the pyrolysis.<sup>44</sup>

$\Delta S$  might indicate the disorder degree of the active complex during pyrolysis. In Figure 7, the average  $\Delta S$  of all the sample is positive. The  $\Delta S$  of untanned sample is 26.99 J/mol, and those for Chestnut-, Tara-, Quebracho-, and Mimosa-tanned leather samples are all positive, that is, 231.8 J/mol, 61.96 J/mol, 306.91 J/mol and 217.57 J/mol, respectively. The  $\Delta S$  is found to be less than 0 for both untanned and Tara-tanned sample at the  $\alpha$  of less than 0.5 and 0.35, respectively, which may be due to the complicated pyrolysis mechanism. There might be a transition state with a more ordered structure in the pyrolysis reaction.<sup>50</sup> Therefore, the  $\Delta S$  can be negative at low conversion, and similar results were obtained in the study of leather tanned with the vegetable tanning agent of fig tree.<sup>19,49</sup> With increasing the conversion, the  $\Delta S$  of the samples increases, suggesting a high reactivity in the later stage of pyrolysis.

## Conclusions

In this study, the pyrolysis kinetic behavior and thermodynamic parameters of leather tanned with different vegetable tanning agents under nitrogen were investigated by TGA at the heating rates of 10, 30, and 50°C/min. The results showed that the pyrolysis process can be divided into three such stages as dehydration, rapid devolatilization, and carbonization. Both methods of FWO and FR were used to investigate the dependence of the  $E_a$  on conversion. The mean  $E_a$  of untanned sample is 191.7- 206.1 kJ/mol. Vegetable tanning increases the  $E_a$  value. The  $E_a$  of Chestnut-tanned leather

is higher than that of Tara-tanned. The difference in  $E_a$  may be due to the differences in the molecular structures. For Quebracho- and Mimosa-tanned leather samples, the  $E_a$  is increased to 333.2-363.8 kJ/mol and 282.7-309.0 kJ/mol respectively. In the  $\alpha$  range from 0.2 to 0.8, the pre-exponential factor ( $A$ ) of the Chestnut- and Tara-tanned leather samples is lower than those of the Quebracho- and Mimosa-tanned leather samples. The average  $\Delta H$ ,  $\Delta G$  and  $\Delta S$  of the four vegetable-tanned samples are all positive while the  $\Delta S$  of the Tara sample appeared negative at the  $\alpha$  of less than 0.35. The difference between the  $E_a$  and  $\Delta H$  is about 5 kJ/mol, which indicated that the pyrolysis of the samples could easily take place. These results of the thermodynamic parameters might provide a reference for the design of the thermochemical conversion processes for vegetable-tanned leather wastes.

## Acknowledgments

This work was supported by the National Natural Science Foundation of China (52073262, 51673177), the Scientific and Technological Project of Ministry of Science and Technology, China (DL2022026006L), and the key Scientific Research Project of Colleges and Universities in Henan Province (21A430034).

## References

1. Gil, R. R., Girón, R. P., Lozano, M. S., Ruiz, B. and Fuente, E.; Pyrolysis of biocollagenic wastes of vegetable tanning. Optimization and kinetic study. *Journal of Analytical and Applied Pyrolysis* **98**, 129-136, 2012.
2. Tahiri S, D. M.; Treatment and valorization of leather industry solid wastes: a review. *JALCA* **104** (02), 52-67, 2009.
3. Vaiopoulou, E. and Gikas, P.; Regulations for chromium emissions to the aquatic environment in Europe and elsewhere. *Chemosphere* **254**, 126876, 2020.
4. DesMarais, T. L. and Costa, M.; Mechanisms of Chromium-Induced Toxicity. *Curr Opin Toxicol* **14**, 1-7, 2019.
5. Sai Bhavya K, S. A., V Samrot A, et al. Leather processing, its effects on environment and alternatives of chrome tanning. *International Journal of Advanced Research In Engineering And Technology* **10** (6), 69-79, 2019.
6. Kanth, S. V., Venba, R., Madhan, B., Chandrababu, N. K. and Sadulla, S.; Cleaner tanning practices for tannery pollution abatement: Role of enzymes in eco-friendly vegetable tanning. *Journal of Cleaner Production* **17** (5), 507-515, 2009.
7. Chojnacka, K., Skrzypczak, D., Mikula, K., Witek-Krowiak, A., Izydorczyk, G., Kuligowski, K., Bandrów, P. and Kulażyński, M.; Progress in sustainable technologies of leather wastes valorization as solutions for the circular economy. *Journal of Cleaner Production* **313**, 127902, 2021.
8. Ma, H., Zhou, J., Hua, L., Cheng, F., Zhou, L. and Qiao, X.; Chromium recovery from tannery sludge by bioleaching and its reuse in tanning process. *Journal of Cleaner Production* **142**, 2752-2760, 2017.

9. Barra Hinojosa, J. and Marrufo Saldaña, L.; Optimization of Alkaline Hydrolysis of Chrome Shavings to Recover Collagen Hydrolysate and Chromium Hydroxide. *Leather and Footwear Journal* **20** (1), 15-28, 2020.
10. Fang, C., Jiang, X., Lv, G., Yan, J. and Deng, X.; Nitrogen-containing gaseous products of chrome-tanned leather shavings during pyrolysis and combustion. *Waste Manag* **78**, 553-558, 2018.
11. Kluska, J., Ochnio, M., Kardas, D. and Heda, L.; The influence of temperature on the physicochemical properties of products of pyrolysis of leather-tannery waste. *Waste Manag* **88**, 248-256, 2019.
12. Hu, Y., Liu, J., Luo, L., Li, X., Wang, F. and Tang, K.; Kinetics and mechanism of thermal degradation of aldehyde tanned leather. *Thermochimica Acta* **691**, 178717, 2020.
13. Guan, Y., Liu, C., Peng, Q., Zaman, F., Zhang, H., Jin, Z., Wang, A., Wang, W. and Huang, Y.; Pyrolysis kinetics behavior of solid leather wastes. *Waste Manag* **100**, 122-127, 2019.
14. Zhang, Z., Hu, Y., Wang, F., Zheng, X., Liu, J. and Tang, K.; Pyrolysis of sulfuric acid-treated chrome-tanned leather wastes: Kinetics, mechanism and evolved gas analysis. *Waste Manag* **143**, 105-115, 2022.
15. Beltrán-Prieto, J. C., Veloz-Rodríguez, R., Pérez-Pérez, M. C., Navarrete-Bolaños, J. L., Vázquez-Nava, E., Jiménez-Islas, H. and Botello-Álvarez, J. E.; Chromium recovery from solid leather waste by chemical treatment and optimisation by response surface methodology. *Chemistry and Ecology* **28** (1), 89-102, 2012.
16. Liu, J., Luo, L., Hu, Y., Wang, F., Zheng, X. and Tang, K.; Kinetics and mechanism of thermal degradation of vegetable-tanned leather fiber. *Journal of Leather Science and Engineering* **1** (1), 1-13, 2019.
17. Sebestyén, Z., Jakab, E., Badea, E., Barta-Rajnai, E., Şendrea, C. and Czégény, Z.; Thermal degradation study of vegetable tannins and vegetable tanned leathers. *Journal of Analytical and Applied Pyrolysis* **138**, 178-187, 2019.
18. Onem, E., Yorgancioglu, A., Karavana, H. A. and Yilmaz, O.; Comparison of different tanning agents on the stabilization of collagen via differential scanning calorimetry. *Journal of Thermal Analysis and Calorimetry* **129** (1), 615-622, 2017.
19. Hu, Y., Liu, J., Li, X., Wang, F., Luo, L., Pei, Y., Lei, Y. and Tang, K.; Assessment of the pyrolysis kinetics and mechanism of vegetable-tanned leathers. *Journal of Analytical and Applied Pyrolysis* **164**, 105502, 2022.
20. Carşote, C., Badea, E., Miu, L. and Gatta, G. D.; Study of the effect of tannins and animal species on the thermal stability of vegetable leather by differential scanning calorimetry. *Journal of Thermal Analysis and Calorimetry* **124** (3), 1255-1266, 2016.
21. Gao, D., Wang, P., Shi, J., Li, F., Li, W., Lyu, B. and Ma, J.; A green chemistry approach to leather tanning process: Cage-like octa(aminosilsesquioxane) combined with Tetrakis(hydroxymethyl) phosphonium sulfate. *Journal of Cleaner Production* **229**, 1102-1111, 2019.
22. Masawat, N., Atong, D. and Sricharoenchaikul, V.; Thermo-kinetics and product analysis of the catalytic pyrolysis of Pongamia residual cake. *J Environ Manage* **242**, 238-245, 2019.
23. Vyazovkin, S., Burnham, A. K., Criado, J. M., Pérez-Maqueda, L. A., Popescu, C. and Sbirrazzuoli, N.; ICTAC Kinetics Committee recommendations for performing kinetic computations on thermal analysis data. *Thermochimica Acta* **520** (1-2), 1-19, 2011.
24. Doyle, C. D.; Series approximations to the equation of thermogravimetric data. *Nature* **207** (4994), 290-291, 1965.
25. Sun, C., Li, C., Tan, H. and Zhang, Y.; Synergistic effects of wood fiber and polylactic acid during co-pyrolysis using TG-FTIR-MS and Py-GC/MS. *Energy Conversion and Management* **202**, 112212, 2019.
26. Wang, B., Xu, F., Zong, P., Zhang, J., Tian, Y. and Qiao, Y.; Effects of heating rate on fast pyrolysis behavior and product distribution of Jerusalem artichoke stalk by using TG-FTIR and Py-GC/MS. *Renewable Energy* **132**, 486-496, 2019.
27. Fong, M. J. B., Loy, A. C. M., Chin, B. L. F., Lam, M. K., Yusup, S. and Jawad, Z. A.; Catalytic pyrolysis of *Chlorella vulgaris*: Kinetic and thermodynamic analysis. *Bioresour Technol* **289**, 121689, 2019.
28. Ahmad, M. S., Mehmood, M. A., Liu, C. G., Tawab, A., Bai, F. W., Sakdaronnarong, C., Xu, J., Rahimuddin, S. A. and Gull, M.; Bioenergy potential of *Wolffia arrhiza* appraised through pyrolysis, kinetics, thermodynamics parameters and TG-FTIR-MS study of the evolved gases. *Bioresour Technol* **253**, 297-303, 2018.
29. Zhang, Y., Chen, Z., Liu, X., Shi, J., Chen, H. and Gong, Y.; SEM, FTIR and DSC Investigation of Collagen Hydrolysate Treated Degraded Leather. *Journal of Cultural Heritage* **48**, 205-210, 2021.
30. Movasaghi, Z., Rehman, S. and ur Rehman, D. I.; Fourier Transform Infrared (FTIR) Spectroscopy of Biological Tissues. *Applied Spectroscopy Reviews* **43** (2), 134-179, 2008.
31. Chen, X., Zhou, L., Xu, H., Yamamoto, M., Shinoda, M., Tada, I., Minami, S., Urayama, K. and Yamane, H.; The structure and properties of natural sheep casing and artificial films prepared from natural collagen with various crosslinking treatments. *Int J Biol Macromol* **135**, 959-968, 2019.
32. Grasel Fdos, S., Ferrao, M. F. and Wolf, C. R.; Development of methodology for identification the nature of the polyphenolic extracts by FTIR associated with multivariate analysis. *Spectrochim Acta A Mol Biomol Spectrosc* **153**, 94-101, 2016.
33. Gao, D., Cheng, Y., Wang, P., Li, F., Wu, Y., Lyu, B., Ma, J. and Qin, J.; An eco-friendly approach for leather manufacture based on P(POSS-MAA)-aluminum tanning agent combination tannage. *Journal of Cleaner Production* **257**, 120546, 2020.
34. Kirkok S K, K. J. K., Kinyanjui T K. A Mechanistic Formation of Phenolic and Furan-Based Molecular Products from Pyrolysis of Model Biomass Components. *Progress in Chemical and Biochemical Research* **5** (4), 376-390, 2022.
35. Liu, J., Luo, L., Zhang, Z., Hu, Y., Wang, F., Li, X. and Tang, K.; A combined kinetic study on the pyrolysis of chrome shavings by thermogravimetry. *Carbon Resources Conversion* **3**, 156-163, 2020.
36. Zhang, J.-h., Kang, G.-j., Yang, H., Liu, Z.-e., Yu, J. and Gao, S.-q.; Co-pyrolysis kinetics and pyrolysis product distribution of various tannery wastes. *Journal of Fuel Chemistry and Technology* **49** (11), 1638-1647, 2021.

37. Balasundram, V., Ibrahim, N., Kasmani, R. M., Hamid, M. K. A., Isha, R., Hasbullah, H. and Ali, R. R.; Thermogravimetric catalytic pyrolysis and kinetic studies of coconut copra and rice husk for possible maximum production of pyrolysis oil. *Journal of Cleaner Production* **167**, 218-228, 2017.
  38. Eimontas, J., Yousef, S., Striūgas, N. and Abdelnaby, M. A.; Catalytic pyrolysis kinetic behaviour and TG-FTIR-GC-MS analysis of waste fishing nets over ZSM-5 zeolite catalyst for caprolactam recovery. *Renewable Energy* **179**, 1385-1403, 2021.
  39. Byrne, C. E., D'Alessandro, O. and Deyá, C.; Tara Tannins as a Green Sustainable Corrosion Inhibitor for Aluminum. *Journal of Materials Engineering and Performance* **31** (4), 2918-2933, 2021.
  40. Lim, A. C. R., Chin, B. L. F., Jawad, Z. A. and Hii, K. L.; Kinetic Analysis of Rice Husk Pyrolysis Using Kissinger-Akahira-Sunose (KAS) Method. *Procedia Engineering* **148**, 1247-1251, 2016.
  41. Varma, A. K., Singh, S., Rathore, A. K., Thakur, L. S., Shankar, R. and Mondal, P.; Investigation of kinetic and thermodynamic parameters for pyrolysis of peanut shell using thermogravimetric analysis. *Biomass Conversion and Biorefinery* **12**, 4877-4888, 2022.
  42. Cai, J. M. and Bi, L. S.; Kinetic analysis of wheat straw pyrolysis using isoconversional methods. *Journal of Thermal Analysis and Calorimetry* **98** (1), 325-330, 2009.
  43. Vyazovkin, S.; Modification of the integral isoconversional method to account for variation in the activation energy. *Journal of Computational Chemistry* **22** (2), 178-183, 2001.
  44. Galvan, D., Orives, J. R., Coppo, R. L., Silva, E. T., Angilelli, K. G. and Borsato, D.; Determination of the Kinetics and Thermodynamics Parameters of Biodiesel Oxidation Reaction Obtained from an Optimized Mixture of Vegetable Oil and Animal Fat. *Energy & Fuels* **27** (11), 6866-6871, 2013.
  45. Ahmad, M. S., Mehmood, M. A., Taqvi, S. T. H., Elkamel, A., Liu, C. G., Xu, J., Rahimuddin, S. A. and Gull, M.; Pyrolysis, kinetics analysis, thermodynamics parameters and reaction mechanism of Typha latifolia to evaluate its bioenergy potential. *Bioresour Technol* **245** (Pt A), 491-501, 2017.
  46. Turmanova, S. C., Genieva, S. D., Dimitrova, A. S. and Vlaev, L. T.; Non-isothermal degradation kinetics of filled with rice husk ash polypropylene composites. *Express Polymer Letters* **2** (2), 133-146, 2008.
  47. Vlaev, L. T., Georgieva, V. G. and Genieva, S. D.; Products and kinetics of non-isothermal decomposition of vanadium(IV) oxide compounds. *Journal of Thermal Analysis and Calorimetry* **88** (3), 805-812, 2007.
  48. Ahmad, M. S., Klemeš, J. J., Alhumade, H., Elkamel, A., Mahmood, A., Shen, B., Ibrahim, M., Mukhtar, A., Saqib, S., Asif, S. and Bokhari, A.; Thermo-kinetic study to elucidate the bioenergy potential of Maple Leaf Waste (MLW) by pyrolysis, TGA and kinetic modelling. *Fuel* **293**, 120349, 2021.
  49. Tabal, A., Barakat, A., Aboukhas, A. and El harfi, K.; Pyrolysis of ficus nitida wood: Determination of kinetic and thermodynamic parameters. *Fuel* **283**, 119253, 2021.
  50. Ong, L. K., Kurniawan, A., Suwandi, A. C., Lin, C. X., Zhao, X. S. and Ismajli, S.; Transesterification of leather tanning waste to biodiesel at supercritical condition: Kinetics and thermodynamics studies. *The Journal of Supercritical Fluids* **75**, 11-20, 2013.
-